Electronic Supplementary Material (ESI) for Physical Chemistry Chemical Physics.

Supporting Information for

Understanding the different effects of 4*d*-transition metals on the performance of Li-rich cathode Li_2MnO_3 by first-principles

Shiwei Zhang[a], Jianchuan Wang[a,*], Xiaoma Tao[b], Xiangyu Yan[a], Yong Du[a], Hans J. Seifert[c], Ting Lei[a]

[a] State Key Laboratory of Powder Metallurgy, Central South University, 410083, Changsha, China

[b] School of Physical Science and Technology, Guangxi University, 530004, Nanning, China

[c] Institute for Applied Materials, Karlsruhe Institute of Technology, Karlsruhe, 76131, Germany

Corresponding author: * jcw728@126.com

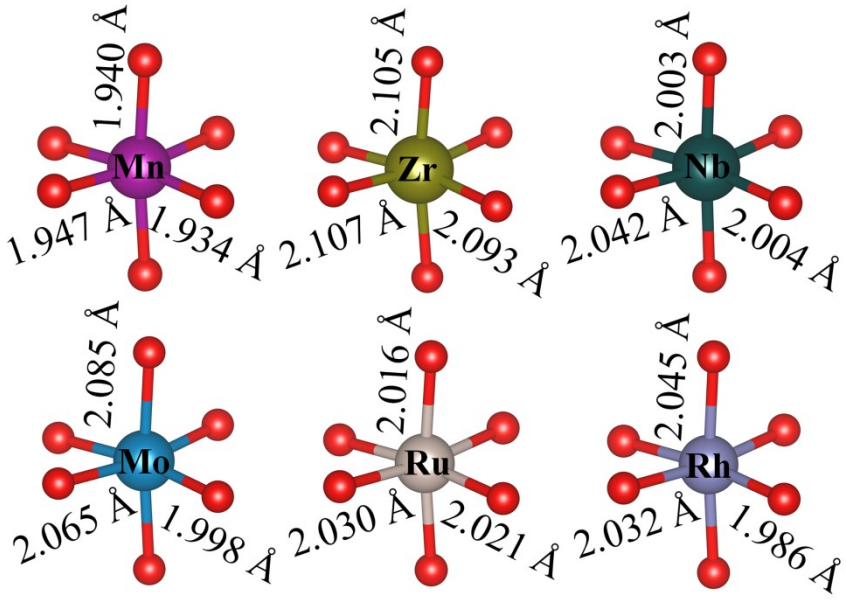

Fig. S1. The bond length of TM-O in TMO_6 octahedron.

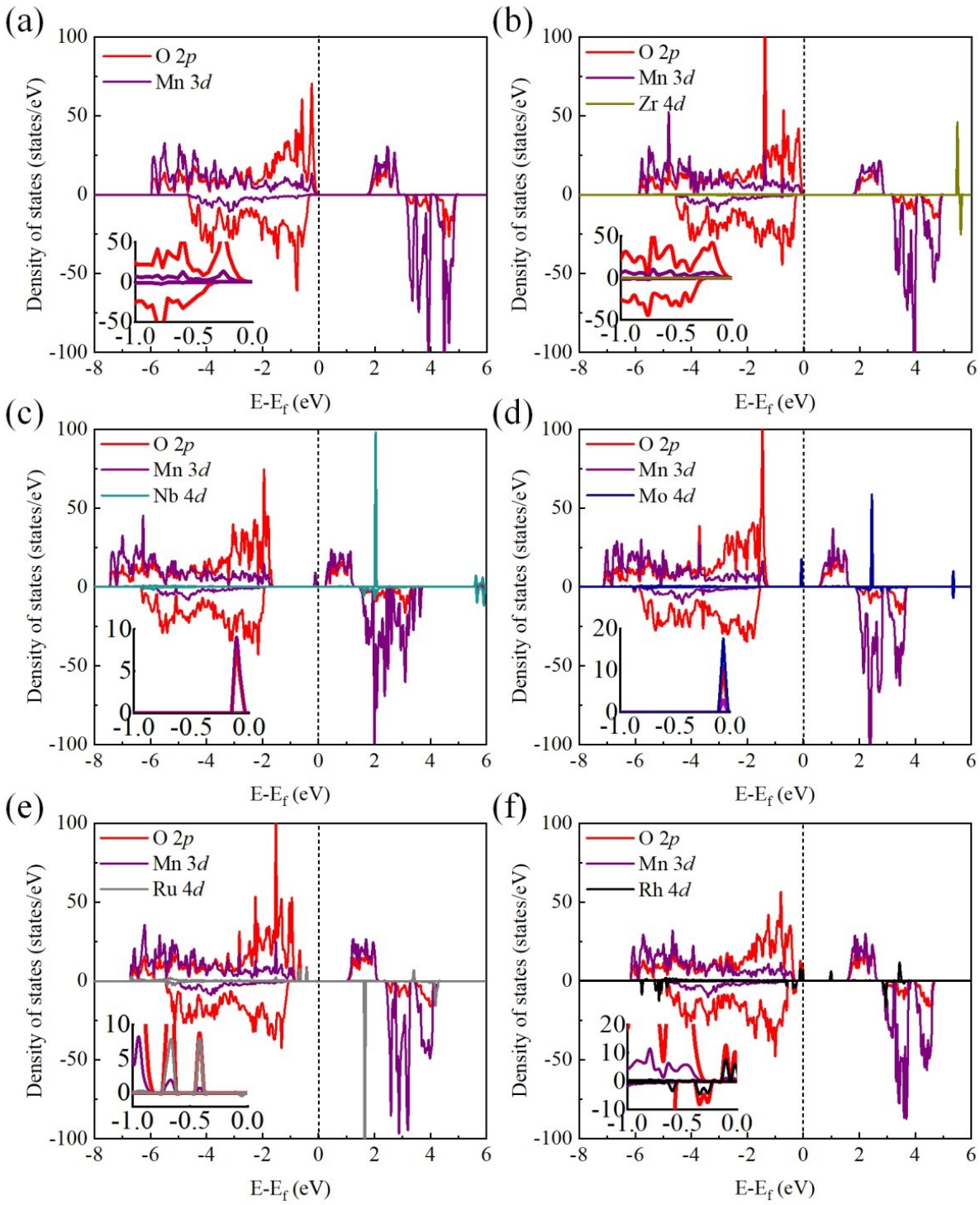

Fig. S2. Density of states of (a) pristine Li_2MnO_3, (b) Zr-Li_2MnO_3, (c) Nb-Li_2MnO_3, (d) Mo-Li_2MnO_3, (e) Ru-Li_2MnO_3 and (f) Rh-Li_2MnO_3. The inset shows an enlarged view ofthe energy range of -0.1 - 0 eV. E_f is the Fermi level, as indicated by the vertical dashed lines.

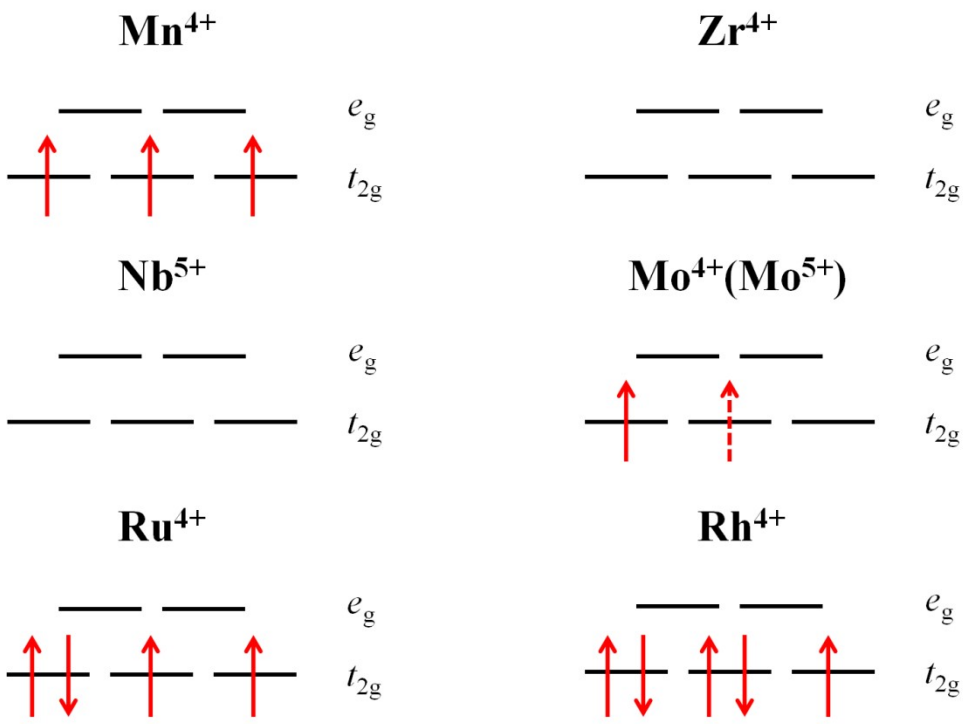

Fig. S3. The electron configuration of Mn in pristine Li_2MnO_3 and the doped TM in TM-Li_2MnO_3.

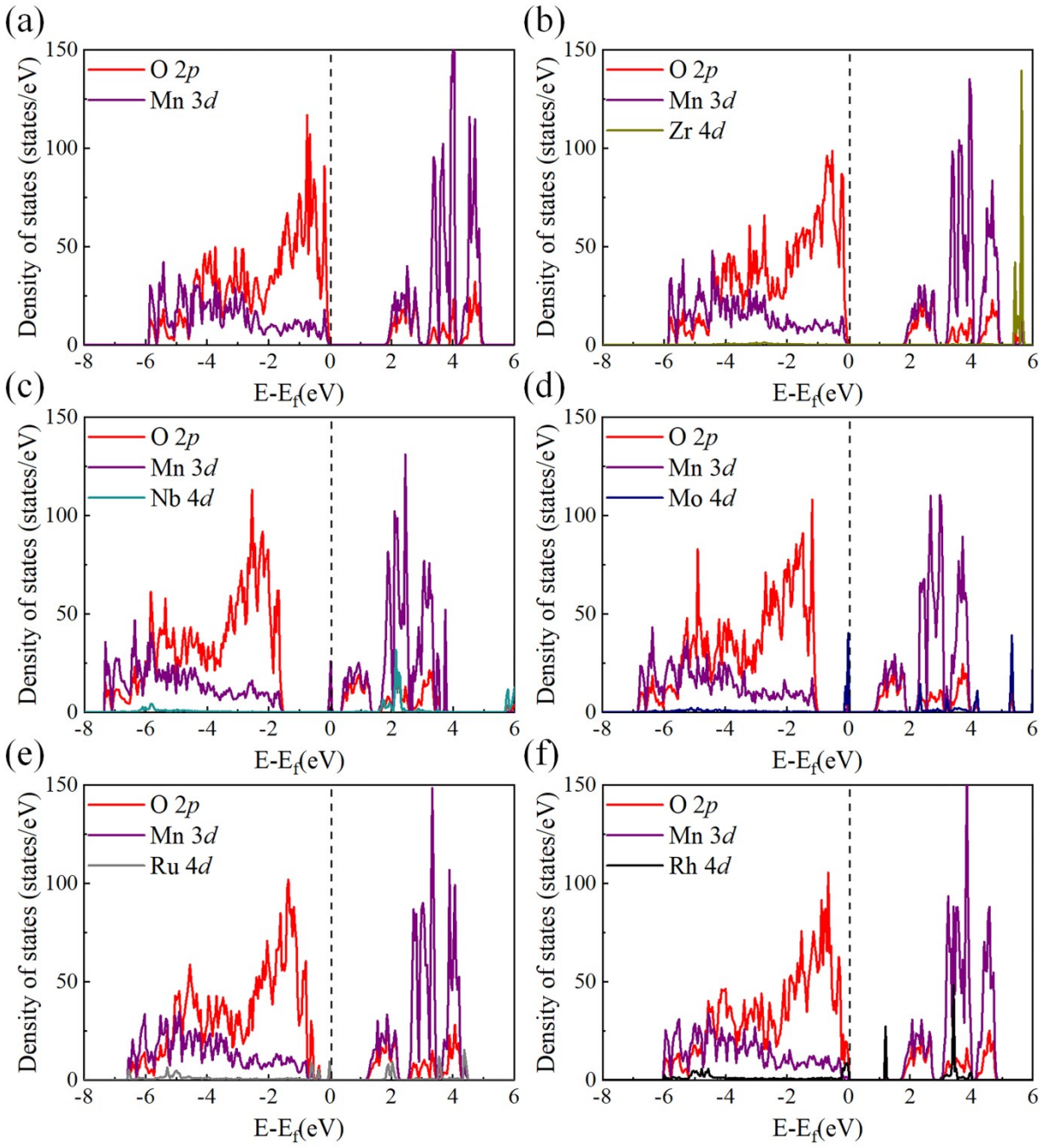

Fig. S4. Density of states with spin-orbital coupling. (a) pristine Li_2MnO_3, (b) Zr-Li_2MnO_3, (c) Nb-Li_2MnO_3, (d) Mo-Li_2MnO_3, (e) Ru-Li_2MnO_3 and (f) Rh-Li_2MnO_3. The vertical dashed lines denote the Fermi level.

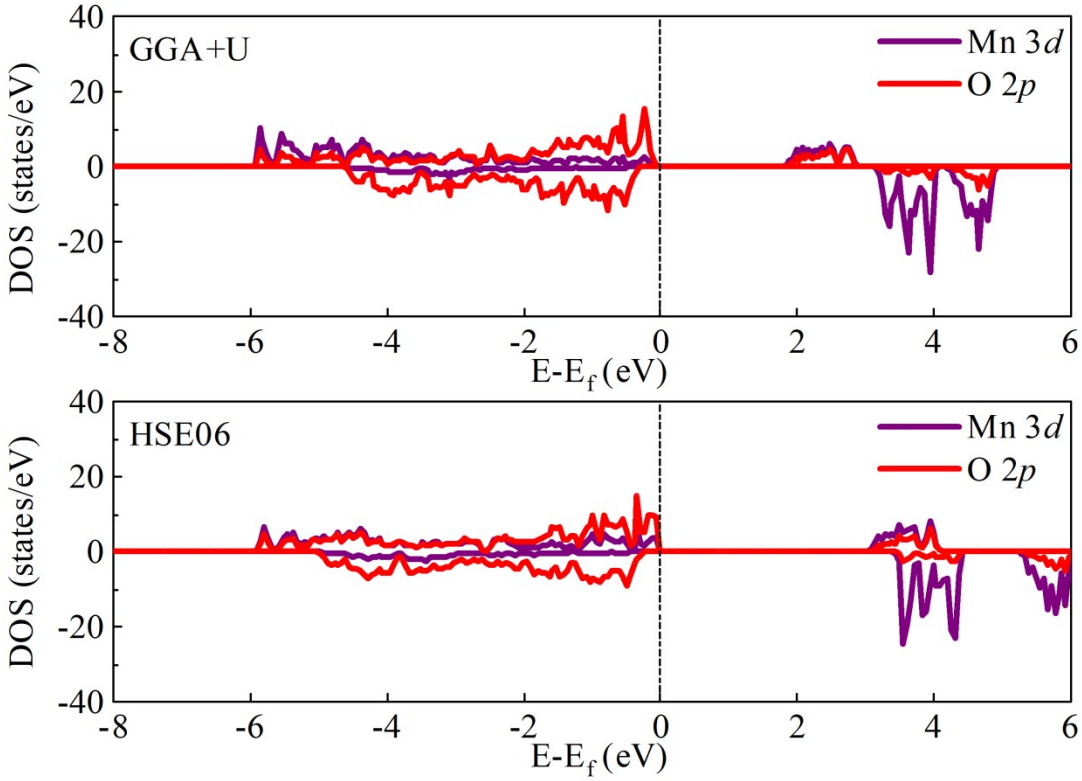

Fig. S5. Density of states of pristine Li_2MnO_3 calculated by GGA+U method and HSE06 method. The vertical dashed lines denote the Fermi level.

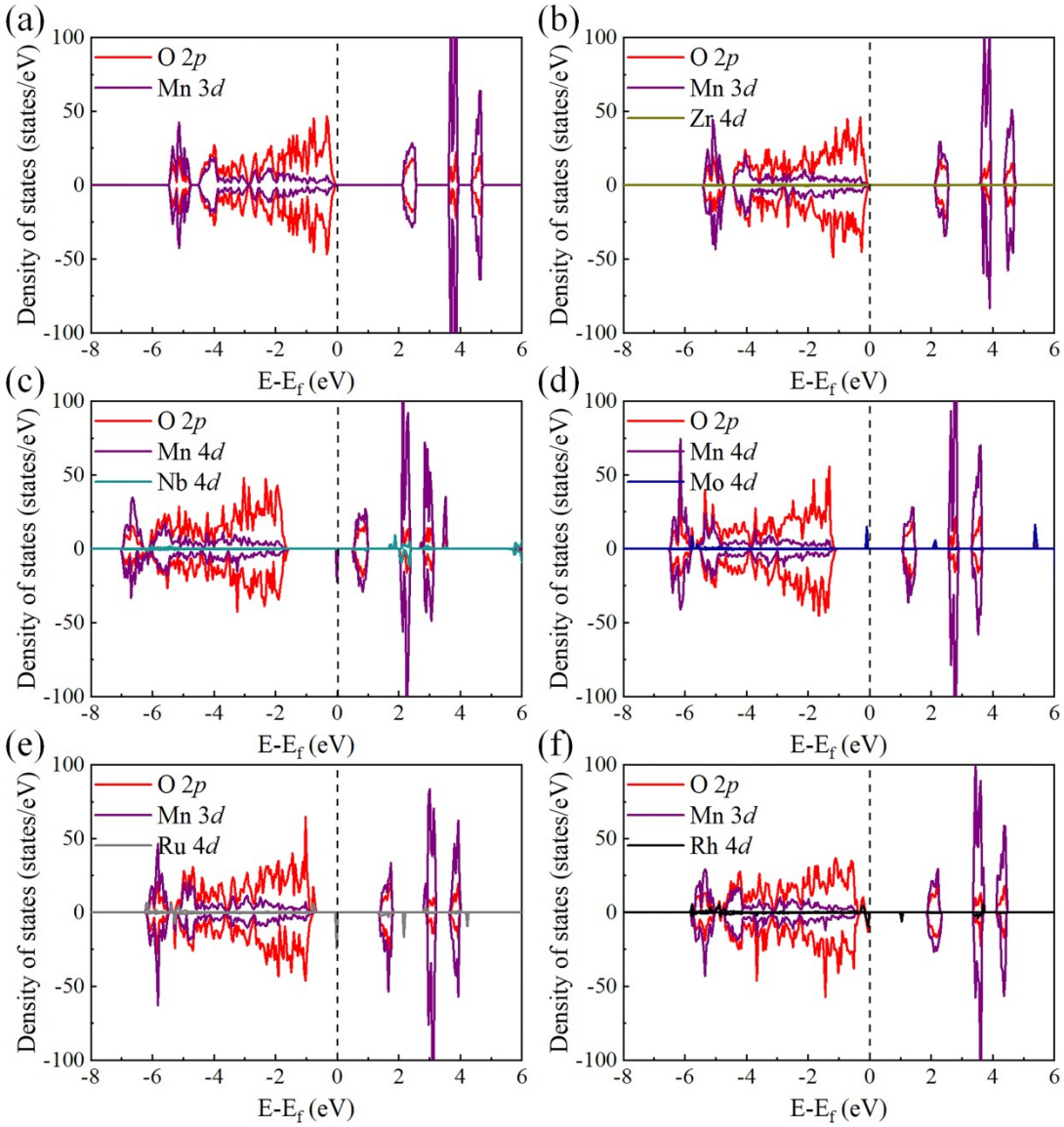

Fig. S6. Density of states of undoped and doped Li_2MnO_3 with antiferromagnetic configuration. (a) pristine Li_2MnO_3, (b) Zr-Li_2MnO_3, (c) Nb-Li_2MnO_3, (d) Mo-Li_2MnO_3, (e) Ru-Li_2MnO_3 and (f) Rh-Li_2MnO_3. The vertical dashed lines denote the Fermi level.

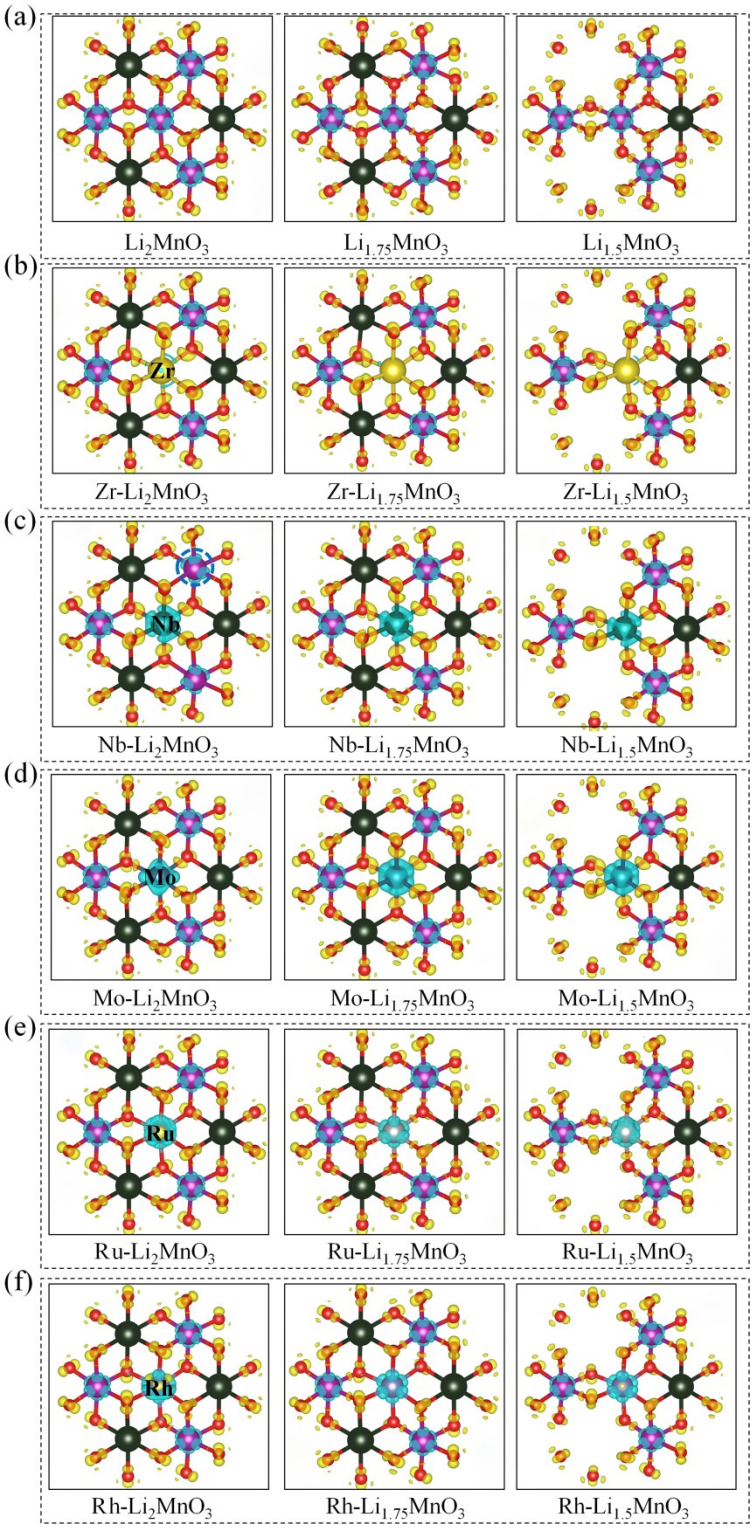

Fig. S7. Three-dimensional charge density differences of (a) pristine Li_2MnO_3, (b) Zr-Li_2MnO_3, (c) Nb-Li_2MnO_3, (d) Mo-Li_2MnO_3, (e) Ru-$Li_2MnO_3$and (f) Rh-Li_2MnO_3 at different delithiaton stages. Yellow zone indicates charge accumulation and blue zone implies charge depletion. The isosurface is 0.03 e/Bohr^3. The black circles indicate the sites where electron-holes are generated.

Table S1. The magnetic moments of Mn and doped TM.

Element	Magnetic moment (μB)
Mn	3.145
Zr	0.008
Nb	0.016
Mo	1.770
Ru	1.646
Rh	0.718

Table S2. The average Bader charges of Mn, doped TM, and O near the TM doping site in TM-Li_2MnO_3 (TM: Zr, Nb, Mo, Ru and Rh).

System	Average Bader charge (e)		
	Mn	O	TM (Zr, Nb, Mo, Ru and Rh)
Li_2MnO_3	+1.848	-1.208	-
Zr-Li_2MnO_3	+1.834	-1.319	+2.534
Nb-Li_2MnO_3	+1.794	-1.279	+2.616
Mo-Li_2MnO_3	+1.838	-1.261	+2.172
Ru-Li_2MnO_3	+1.844	-1.182	+1.689
Rh-Li_2MnO_3	+1.848	-1.151	+1.455

Table S3. The intralayer diffusion barrier E_v of Li during initial delithiation.

System	E_v (eV)	
	Path $2c1 - 4h1$	Path $2c1 - 4h2$
Li_2MnO_3	0.58	0.83
Zr-Li_2MnO_3	0.51	0.88
Nb-Li_2MnO_3	0.53	0.85
Mo-Li_2MnO_3	0.57	0.84
Ru-Li_2MnO_3	0.56	0.82
Rh-Li_2MnO_3	0.57	0.81

Table S4. The intralayer diffusion barrier E_v of Li during further delithiation.

System	E_v (eV)	
	Path$2c1$- $4h1$	Path$2c2$- $4h2$
$Li_{1.5}MnO_3$	0.27	0.48
Zr-$Li_{1.5}MnO_3$	0.22	0.60
Nb-$Li_{1.5}MnO_3$	0.22	0.54
Mo-$Li_{1.5}MnO_3$	0.27	0.52
Ru-$Li_{1.5}MnO_3$	0.24	0.50
Rh-$Li_{1.5}MnO_3$	0.35	0.58

Table S5. The interlayer diffusion barrier E_v of Li on path 2*b* – 4*h*2 during initial and further delithiation.

System	E_v (eV)	
	Initial delithiation	Further delithiation
$Li_{1.5}MnO_3$	0.77	0.21
Zr-$Li_{1.5}MnO_3$	0.64	0.17
Nb-$Li_{1.5}MnO_3$	0.73	0.16
Mo-$Li_{1.5}MnO_3$	0.73	0.17
Ru-$Li_{1.5}MnO_3$	0.66	0.22
Rh-$Li_{1.5}MnO_3$	0.74	0.27